RESEARCH ARTICLE

Cellulose Nanocrystal-Enhanced Thermal-Sensitive Hydrogels of Block Copolymers for 3D Bioprinting

Yuecheng Cui[1], Ronghua Jin[2], Yifan Zhang[3], Meirong Yu[2], Yang Zhou[1], Li-Qun Wang[1,4]*

[1]MOE Key Laboratory of Macromolecular Synthesis and Functionalization, Department of Polymer Science and Engineering, Zhejiang University, Hangzhou 310027, P. R. China
[2]Second Affiliated Hospital of Medical College, Zhejiang University, Hangzhou 310009, P. R. China
[3]Hangzhou Regenovo Biotechnology Co. Ltd, Hangzhou Economic and Technological Development Area, Hangzhou 310018, P. R. China
[4]Hangzhou Medsun Biological Technology Co., Ltd, Hangzhou Economic and Technological Development Area, Hangzhou 310018, P. R. China

Abstract: The hydrogel formed by polyethylene glycol-aliphatic polyester block copolymers is an ideal bioink and biomaterial ink for three-dimensional (3D) bioprinting because of its unique temperature sensitivity, mild gelation process, good biocompatibility, and biodegradability. However, the gel forming mechanism based only on hydrophilic-hydrophobic interaction renders the stability and mechanical strength of the formed hydrogels insufficient, and cannot meet the requirements of extrusion 3D printing. In this study, cellulose nanocrystals (CNC), which is a kind of rigid, hydrophilic, and biocompatible nanomaterial, were introduced to enhance the hydrogels so as to meet the requirements of extrusion 3D printing. First, a series of poly(ε-caprolactone/lactide)-*b*-poly(ethylene glycol)-*b*-poly(ε-caprolactone/lactide) (PCLA-PEG-PCLA) triblock copolymers with different molecular weights were prepared. The thermodynamic and rheological properties of CNC-enhanced hydrogels were investigated. The results showed that the addition of CNC significantly improved the thermal stability and mechanical properties of the hydrogels, and within a certain range, the enhancement effect was directly proportional to the concentration of CNC. More importantly, the PCLA-PEG-PCLA hydrogels enhanced by CNC could be extruded and printed through temperature regulation. The printed objects had high resolution and fidelity with effectively maintained structure. Moreover, the hydrogels have good biocompatibility with a high cell viability. Therefore, this is a simple and effective strategy. The addition of the hydrophilic rigid nanoparticles such as CNC improves the mechanical properties of the soft hydrogels which made it able to meet the requirements of 3D bioprinting.

Keywords: Poly(ε-caprolactone/lactide)-b-poly (ethylene glycol)-*b*-poly(ε caprolactone/lactide); Thermal-sensitive hydrogels; Three-dimensional bioprinting; Cellulose nanocrystal

*Correspondence to: Li-Qun Wang, Department of Polymer Science and Engineering, Zhejiang University, Hangzhou 310027, P. R. China; lqwang@zju.edu.cn

Received: June 02, 2021; **Accepted:** August 03, 2021; **Published Online:** August 27, 2021

Citation: Cui Y, Jin R, Zhang Y, *et al.,* 2021, Cellulose Nanocrystal-Enhanced Thermal-Sensitive Hydrogels of Block Copolymers for 3D Bioprinting. *Int J Bioprint*, 7(4):397. http://doi.org/10.18063/ijb.v7i4.397

1. Introduction

Three-dimensional (3D) bioprinting is a rapid additive manufacturing technology which is used in the field of tissue engineering[1,2]. As an emerging research direction, it has attracted widespread attention. The printing methods in this technology are diverse, and material jetting, material extrusion, and vat polymerization bioprinting are commonly used[3-7]. Among them, material extrusion bioprinting is capable of fabricating more scaled bio-scaffold compared with the other two technologies, exhibiting more potential and prospect in

tissue engineering and other biomedical fields. For the extrusion-based printing, the inks in the cylinder can be extruded under pressure through the nozzle and deposited on a substrate layer by layer. Therefore, the ink not only can be extruded smoothly but also can be set quickly after deposition. The fact that a printable biomaterial is required to have the properties of shear thinning, fast curing and good biocompatibility presents a huge challenge in broadening extrudable biomaterial inks[2,8].

Hydrogels are water-swellable 3D crosslinking network with adaptable mechanical strength. Therefore, under the premise of retaining the original excellent properties of the hydrogel, enhancing its mechanical strength to meet the needs of 3D printing is one of the focuses in this field[9,10]. Nevertheless, the diverse and complex gelation mechanisms of hydrogels are reciprocally restricted with technology condition of extrusion-based printing, thereby restraining the application in 3D bioprinting. Thus, it is an application prospect to develop more extrudable hydrogels with easy gelation mechanism[11,12]. Temperature-responsive hydrogels are the soft materials that can reversibly transit between gel and sol by regulating temperature, which are the ideal printable and extrudable materials[13]. Unfortunately, the crosslinking network of this type of hydrogels is often based on hydrogen bonds or hydrophilic-hydrophobic interactions. The weaker forces lead to poor structural stability and low mechanical strength of the cross-linked networks. Extrusion swelling and even structural collapse will occur during printing[14-16]. Therefore, the present research focuses on enhancing the mechanical strength of the hydrogels while retaining the original excellent properties.

At present, the introduction of carbon-carbon double bonds in the chemical structure of the materials, and subsequently photo-curing is the main means. Among them, methacryloyl gelatin (GelMA) is a representative of this strategy. In this approach, the chemical modification is easy and convenient. The degree of substitution of the double bond can be adjusted while the structure of the gelatin will not change significantly. The printed GelMA object can be fast photo-crosslinking by adding a photoinitiator. The mechanical strength of the cured hydrogel is remarkably enhanced[17-20]. However, the introduction of photoinitiator and its free radical species caused by UV irradiation that causes damage to the cells affect the cell survival rate[21-23]. We previously reported an alternative approach: introducing a crystalline poly(*ε*-caprolactone) (PCL) block into the molecular structure to construct poly(*ε*-caprolactone)-*b*-poly(ethylene glycol)-*b*-poly(*ε*-caprolactone) triblock copolymer. The results showed that the crosslinked network of the copolymers could partially crystalize in water. Compared with the amorphous control group, it showed significantly improved strength and thermal stability, which meets the requirements of extrusion 3D printing[12]. However, the limitation of this method is that the amorphous materials do not have the ability to crystallize. Therefore, it is necessary to develop more extensive mechanical enhancement strategies.

In this study, cellulose nanocrystals (CNC), kind of rigid nanoparticles, were introduced to strengthen the amorphous block copolymer hydrogels. CNC is a rod-shaped rigid nanomaterial made of natural polymers, which has a good biocompatibility and can be stably dispersed into nanoparticles in an aqueous medium[24-27]. As previously reported[28-30], the introduction of CNC could mechanically enhance the hydrogels. Therefore, we hope to introduce such rigid nanomaterials as reinforcing fillers to improve the mechanical strength and printability of amorphous hydrogels. Thus, triblock copolymers, poly(*ε*-caprolactone/lactide)-*b*-poly(ethylene glycol)-*b*-poly(*ε*-caprolactone/lactide) (PCLA-PEG-PCLA), were chosen for the study. A series of PCLA-PEG-PCLA copolymers with different molecular weight were prepared; subsequently, different amounts of CNC were introduced, and the mechanical improvement effect on the hydrogels was evaluated. It is found that the addition of CNC significantly improved the thermal stability and mechanical strength of the hydrogels. Within a certain concentration range, the improvement of hydrogel performance was proportional to the increase of CNC concentration. In addition, when a certain amount CNC was added, the sol system that cannot form a gel state at room temperature has a significant "liquid-solid transition" phenomenon. More importantly, the CNC-enhanced hydrogels could form effectively maintained 3D structural objects with high resolution and fidelity during the printing process, and no extrusion swelling or structural collapse was observed. The strategy of introducing rigid nanoparticles such as CNC to the mechanically weak hydrogels meets the demand of 3D bioprinting, and is a simple and effective way to improve the comprehensive performance of the thermal-sensitive hydrogels.

2. Materials and methods

2.1. Materials

CNC (11 wt%) was purchased from Beijing North Tianchen Technology Co., Ltd. (Beijing, China). *ε*-caprolactone (98%) was received from Shanghai Aladdin Biochemical Technology Co., Ltd. and dehydrated by CaH_2 for more 2 weeks. PEG ($\boldsymbol{M}_n$ = 6 000, 8 000 and 10 000 Da) was purchased from Sigma-Aldrich (98%) and dehydrated by lyophilization. L-lactide (LLA) was synthesized in our lab and recrystallized from ethyl acetate and dried in a vacuum oven at room temperature over 3 days. Stannous octoate ($Sn(Oct)_2$, 95%) and $CDCl_3$ (99.9%) were also obtained from Sigma-Aldrich. All other chemicals were obtained from Shanghai Chemical Reagent Co.

(Shanghai, China) and used without further purification, unless otherwise specified.

2.2. Synthesis of the triblock copolymer

The PCLA-PEG-PCLAs were all synthesized through ring-opening polymerization. Taking PCA_1 as an example, 3 g dihydroxyl PEG (M_n = 6 000 Da, 0.5 mmol), 1.14 g ε-CL (1.11 mL, 10 mmol), 1.44 g LLA (10 mmol), and 3% Sn $(Oct)_2$ were added into a blank round-bottom flask. The mixture was melted at 60°C and then purified with argon under stirring for 3 times. The polymerization was conducted under vacuum at 160°C for 8 h. The reaction was terminated at –20°C. The obtained crude product was dissolved in around 5 mL CH_2Cl_2 and precipitated in over 100 mL diethyl ether for 3 times. The solid product was then dried in a vacuum oven overnight.

2.3. Characterization of copolymer structure

^{1}H NMR spectra of triblock copolymers were recorded using a Brucker Avance-400 nuclear magnetic resonance instrument. The solvent was $CDCl_3$. The gel permeation chromatography (GPC) was determined through Waters PL-GPC-50 instrument. The eluent was THF with a flow rate of 1.0 mL/min.

2.4. Vial-inverting test

The enhancement effect of CNC on phase transition of hydrogels was evaluated by vial-inverting test. The hydrogels of the copolymers were prepared at the concentration of 20 wt% while 0, 2.2, 4.4, and 8.8 wt% CNC were used. The vials were incubated in a water bath. The temperature was regulated from 25 to 70°C with an increment of 1°C per step. Each sample was equilibrated for 5 min at each temperature and the state was evaluated. Once a flowable or dehydrated state was observed after inverting the vial, the transition temperature would be recorded.

2.5. Rheological experiments

The rheological properties of hydrogels were characterized through a TA ARES-G2 instrument using a 25 mm parallel plate geometry. The samples were loaded on the Peltier platform. Temperature sweep experiments were conducted at 1 Hz from 25 to 75°C with a ramp rate of 3°C/min. Frequency sweep experiments were carried out at 25°C from 0.1 to 100 rad/s with a strain value of 0.5%. Strain sweep experiments (25°C) were performed at a strain ranging from 0.01% to 1000% with a frequency value of 1 Hz. Shear thinning tests was carried out at 37°C with a frequency value of 1 Hz. The shear rates were from 0.01 to 100 rad/s. The thixotropy experiments (25°C) were performed at an alternating strain of 0.01% and 100% for 100 s, respectively, per cycle.

2.6. Scanning electron microscopy (SEM)

The copolymers-formed hydrogels (20 wt%) were lyophilized at -50°C under 10 Pa (Vacuum freeze dryer, FD-1A-50, BiLon, Shanghai, China) overnight, which was followed by metal-spraying using an MSP-2S, an ion sputtering instrument (EIKO Corporation, Japan) for 1 min. The SEM images were obtained through a Hitachi S-4800 SEM instrument.

2.7. Degradation properties

20 wt% PCA_2 hydrogel was chosen to study the degradation properties. 0.5 g of PCA_2 was added to a vial and 1 mL phosphate buffer (PB) containing 0.1 mg lipase (Aladdin, Shanghai, China) was subsequently added. The experiments were conducted in triplicates at 37°C and the buffer was refreshed every day. The residual samples were taken out and lyophilized at specific time intervals. The weight of each sample was recorded and the average value of weight ratio of weight loss and the original weight before incubation was calculated as the degradation rate for the analysis.

2.8. 3D printability of hydrogels

The extrusion-based 3D printing was carried out with an instrument of Bio-Architect® PRO (Regenovo). The hydrogels were filled into the barrels and then placed into an oven at 37°C overnight to eliminate the bubbles. The corresponding GCodes and software were supported by Regenovo. The filament collapse experiments and micro-extrusion were performed by adjusting the nozzle size, the pneumatic pressure value, and translational speed. Taking the 20 wt% PCA_2+4.4 wt% CNC gel with the 0.41 mm of nozzle as an example, the thickness was set as 0.4 mm and the 3D constructs were printed at 37°C under 0.3 MPa of air pressure with 10 mm/s of transitional speed.

2.9. *In vitro* cytotoxicity assay

Primary human fibroblasts (HDFs) were used for evaluation. HDFs were obtained from discarded human foreskin and used until 4–6th passage. The cell seeding density was 500/well. The Dulbecco's modified Eagle's medium, Sigma, USA was used as culture medium.

The cytocompatibility of the copolymers with different concentrations was evaluated through staining with cytotoxicity assay kit (KeyGEN BioTECH, China). The culture medium was removed and washed with PB saline (PBS) for 3 times. The work solution (0.5 μL propidium iodide (PI) + 0.5 μL calcein acetoxymethyl ester (AM) in 1 mL PBS) was added into the samples and then incubated for 45 min at room temperature. The fluorescent images were observed through fluorescence microscope (Leica, Germany); the living and dead cells showed as green and red regions, respectively.

The cytocompatibility of hydrogels was also investigated. 20 wt% PCA_2+4.4 wt% hydrogel was chosen for the investigation while cells were seeded on its surface. The following process was identical to the previous procedure. The fluorescent images were captured after 12-h co-incubation.

(c) The cell viability was also carried out using Cell Counting Kit-8 (CCK-8) cell viability assay. The CCK-8 stock solution (Dojindo, Kumamoto, Japan) was diluted (1:10) in culture medium to form a working solution. The human primary fibroblasts and copolymer at a given concentration were submerged for 2 h. 100 μL of the submerged solution was extracted and transferred into a plate of 96 wells. The measurements were conducted using a microplate reader (BioTek Instrument, USA) with the absorbance at 450 nm. The samples were washed with PBS until the working solution was totally removed; and fresh medium was added subsequently for incubation.

3. Results and discussion

3.1. Synthesis and properties of the copolymers

According to our previous study, dihydroxy terminated PEGs with different molecular weight (6, 8, and 10 kDa) were chosen as the macroinitiator. By regulating the feed ratio, the molecular weight of polyester was controlled around 2 kDa. Thus, three PCLA-PEG-PCLA copolymers with different chain lengths, named, respectively, as PCA_1, PCA_2 and PCA_3, were prepared via ring-opening polymerization using $Sn(Oct)_2$ as the catalyst (**Figure 1**). To ensure the elimination of the intrinsic crystallinity of polyester, the constitutional repeating unit between caprolactone (CL) and lactide (LA) were adjusted to the same molar number. The obtained samples were characterized through ^{1}H NMR and GPC, which is shown in **Table 1**. Through the calculation of integral area in ^{1}H NMR spectra (**Figure 2A**), the chain length of each polyester block was around 2000 Da. That means the block ratio of polyester decreased with the increase of PEG chains. Meanwhile, the molar ratio of the constitutional repeating unit between CL and LA was calculated, respectively, as 0.98, 0.9, and 1.08, which were close to the equal distribution of 1:1, ensuring the amorphous state of the hydrophobic block. In addition, the GPC results illustrated that the molecular weight of all copolymers was narrowly distributed (**Figure 2B**).

3.2. Gel-sol transition of the CNC-enhanced copolymer gels

The hydrogels formed by these copolymers exhibited thermal-sensitive properties with gel-sol transition, that is, these gels have a lower critical gelation temperature (LCGT). As the temperature is lower than LCGT, the system is in a gel state. When the temperature is above LCGT, lower concentration gels transform into a flowable sol state and the gels of higher concentration will dehydrate and precipitate. Therefore, LCGT can effectively reflect the thermal stability of the hydrogels. Since the polyester block is an amorphous block formed by the copolymerization of two monomers, the formed hydrogel often has a low LCGT and is not as stable as a gel formed by a crystalline copolymer with the same molecular weight. Thus, CNCs with different concentrations were introduced to the hydrogels (20 wt%) to evaluate the enhancement effect (**Figure 3A**). It can be seen that the overall LCGT was at a relatively low level in the absence of CNC, and as the molecular weight of PEG increases, the LCGT gradually decreases. The reduction of hydrophobic block ratio will be detrimental to the thermal stability of gels, which is consistent with our previous study[16]. The thermal stability of the hydrogels is improved to varying degrees when different concentrations of CNC

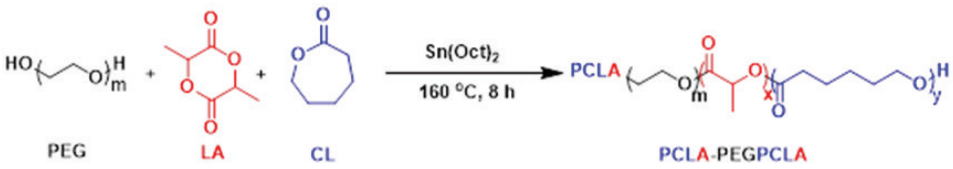

Figure 1. The synthesis strategy of PCLA-PEG-PCLA triblock copolymers.

Table 1. Properties of PCLA-PEG-PCLA triblock copolymers

Samples	$M_{n,NMR}$ [a,c]	$M_{n,GPC}$ [b]	M_w/M_n [b]	Polyester/PEG[a] (M_n/M_n)	CL/LA[a] (mol/mol)
PCA_1	2 170-6 000-2 170	10 500	1.01	0.72	0.98
PCA_2	1 820-8 000-1 820	13 400	1.11	0.46	0.9
PCA_3	1 880-10 000-1 880	16 100	1.25	0.38	1.08

[a]$M_{n,NMR}$, polyester/PEG ratios and CL/LA ratios of the copolymers were calculated from 1H NMR spectra. [b]$M_{n,GPC}$ and M_w/M_n of copolymers were calculated by GPC. [c]The difference among the PCA_1, PCA_2 and PCA_3 was the molecular weight of PEG, which was 6, 8, and 10 kDa, respectively, while the hydrophobic block was kept at around 2 kDa for the convenience of subsequent comparison

(2.2, 4.4, and 8.8 wt%, respectively) were added to the hydrogels. Among them, the effect on PCA_3 is the most remarkable. When the concentration of CNCs reaches 8.8 wt%, the LCGT of PCA_3 increased by about 15°C, showing a notable promotion effect.

This enhancement effect on phase transition with different concentrations of CNC also shows a similar result in tan δ (**Figure 3B**). Taking PCA_2 samples (20 wt%) as an example, temperature sweep was conducted ranging from 25 to 75°C. It can be found that tan δ of four samples increased from gel state (tan δ < 1, G' > G'') to sol state (tan δ > 1, G' < G'') with the increment of temperature, exhibiting a typical thermal-sensitive effect. As the temperature increased further (T >60°C), tan δ decreased due to the dehydration of hydrogels at elevated temperature. Compared with the PCA_2 without CNC, the tan δ reduced to varying degrees after different concentrations of CNC were added. As 8.8 wt% CNC was added, the values of tan δ became far below 1, showing a strong elastic effect. These results demonstrate that the introduction of CNCs can effectively improve the thermal stability of the crosslinked network of the copolymers.

3.3. Rheological properties of the CNC-enhanced hydrogels

Considering that the addition of different concentrations of CNCs has an effect on the thermal stability of the hydrogels to varying degrees, it is thereby predictable that the mechanical strength of the hydrogels may be similarly enhanced by CNC. Therefore, the rheological properties of the copolymers were investigated. Frequency sweep was conducted (**Figure 4**). For PCA_1 and PCA_2, the addition of CNCs significantly improved the modulus of the hydrogel, and with the increase of CNC concentration, the increased effect on the hydrogel strength becomes more prominent. For PCA_3 samples, the gel modulus is substantially improved after adding CNCs. From the results, it can be seen that the PCA_3 without CNC showed a high degree of frequency dependence. That is, the storage modulus (G') < loss modulus (G'') in the low frequency range (0.1~10 rad/s), and in the high frequency range (10~100 rad/s), it became G' > G'', indicating that PCA_3 (~20 wt%) can hardly form a stable hydrogel at room temperature, which is consistent with the above phase diagram (**Figure 3A**). Longer PEG chain is detrimental to gel formation. As the CNC concentration increase to 2.2 wt% in the gel system, the gel point moves to lower frequency, from 10 rad/s to 2 rad/s. Broader frequencies range was facilitated for gel formation. When the CNC concentration reached 4.4 wt%, a typical "gel-sol transition" could be observed where G' > G'' within the whole given frequencies range, but the sample still showed a significant frequency dependence. When the CNC concentration reached 8.8 wt%, the gel modulus was further improved, and the variation of gel modulus on frequency became inconspicuous, exhibiting a more elastic effect.

According to the results of frequency sweep, the addition of CNCs remarkably improves the gel modulus, and the improvement effect is proportional to the CNC concentration. For those samples which cannot form stable gels under conventional conditions, the addition of CNC can facilitate the gel point to shift to lower frequencies, exhibiting an elastic effect at a wider frequency range. When the CNC concentration reaches a certain extent, "gel-sol" transition effect will occur. According to our previous research, the hydrophilic block ratio of copolymers was higher within a certain range, and the hydrophobic cores were smaller while the hydrophilic chains were longer. Thus, the effective crosslinking points between micelles would reduce. The crosslinking network would thereby become unstable and exhibit frequency dependence, especially in the lower frequencies range. Due to the hydrophilic group (e.g. hydroxyl group) on the CNC surface, more hydrogen bonds would be generated between CNC and PEG chain. Thus, the effective crosslinking points increase remarkably, leading to a more stable structure of the network. That is, the CNC enhanced hydrogels show more independent on the frequency compared with the unmodified gels. Thereby, the stability of gels would improve[30-35].

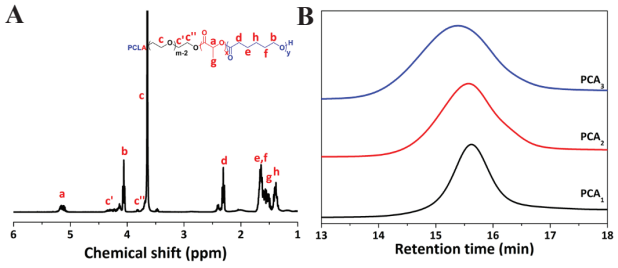

Figure 2. (A) $_1$H NMR spectra of PCLA-PEG-PCLA. The solvent used was D_2O. (B) GPC spectra of PCA_1, PCA_2 and PCA_3. The solvent used was THF.

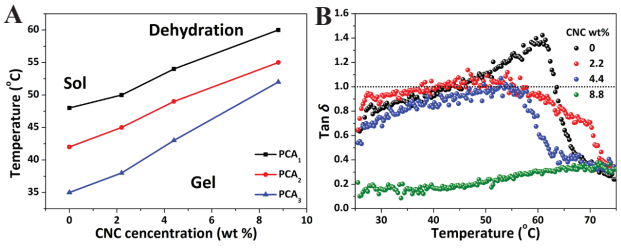

Figure 3. Enhancement effect of CNC on phase transition. (A) Phase diagram of PCLA-PEG-PCLA hydrogels (20 wt%) with CNC of different concentrations. (B) Tan δ of PCA_2 hydrogels added with different concentrations of CNC as a function of temperature with a ramp rate of 3°C/min.

The strain sweep was subsequently conducted and the results are shown in **Figure 5**. Abiding by the rule of normal crosslinking system, all the samples of the three groups had a linear viscoelastic regime in which the gel modulus had no significant change and $G' > G''$, showing a typical elastic effect. When the strain reached a certain extent, the hydrogel yields and modulus drop abruptly, and $G' < G''$, exhibiting a liquid-like state. Moreover, we observed that there were significant changes between before and after the addition of CNC under the large amplitude oscillatory strain (LAOS). The system with added CNC at the LAOS produced an obvious weak strain overshoot (WSO) phenomenon, that is, when the gel yielded, G'' experienced a sharp rise first and then abruptly decrease. We believe that this is due to the destruction and reorganization of the cross-linked network structure in the process of increasing strain amplitude, resulting in a sudden increase in energy dissipation. The system without CNC has no significant WSO phenomenon, and with the increase of CNC concentration, the WSO phenomenon becomes more obvious, indicating that this phenomenon is attributed to the addition of CNC, and the copolymer itself has an amorphous structure in the water phase. The energy dissipation in the LAOS process is not obvious, and WSO does not occur. However, the introduced CNC itself is a rigid and crystalline material. The energy dissipation required for the destruction and reorganization of its structure in the same LAOS process rises sharply, and with the increase of CNC content, the WSO phenomenon becomes more apparent. The addition of CNC significantly increases the modulus of the system, and the modulus increases with the increase of CNC concentration, which is consistent with the previous results[16,36-39].

The rheological results effectively illustrate that the introduction of CNC can not only increase the effective crosslinking chains of the hydrogels but also enhance the structural stability of the network due to its rigid crystal particles. Thus, enhanced hydrogels will weaken the frequency dependence and simultaneously strengthen the mechanical properties.

3.4. Printability of CNC-enhanced hydrogel

According to the thermodynamic and rheological results, the addition of CNCs effectively improves the thermal stability and mechanical strength of hydrogels. It is thereby believed that printability can also be improved. Thus, 20 wt% PCA_2+4.4 wt% CNC was chosen for the investigation of the feasibility in 3D bioprinting (**Figure 6**). Extrudability was first evaluated. As mentioned above, materials with shear-thinning properties can be extruded. Thus, the viscosity variation of the hydrogel ranging from 0.01 to 100 rad/s was investigated and the result is shown in **Figure 6A**. It is found that the viscosity of the sample experienced a

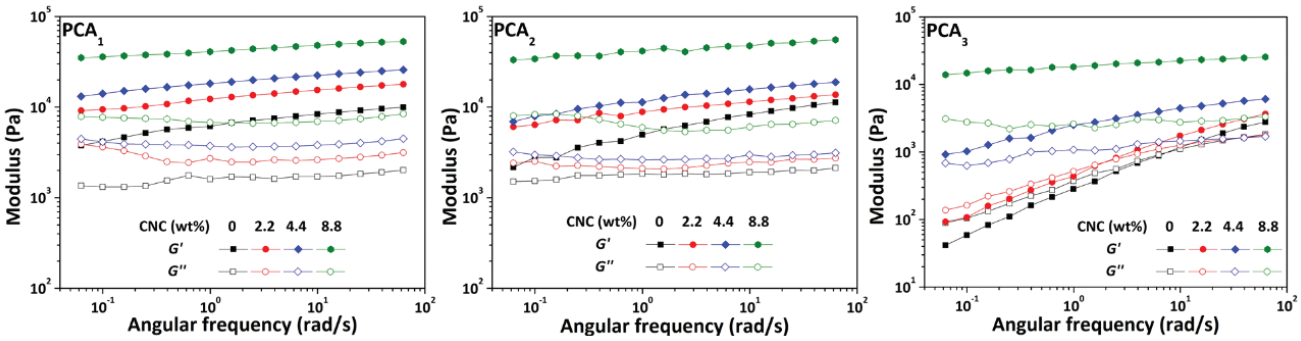

Figure 4. Frequency sweep of PCA_1, PCA_2 and PCA_3 (20 wt%) with CNC of different concentrations.

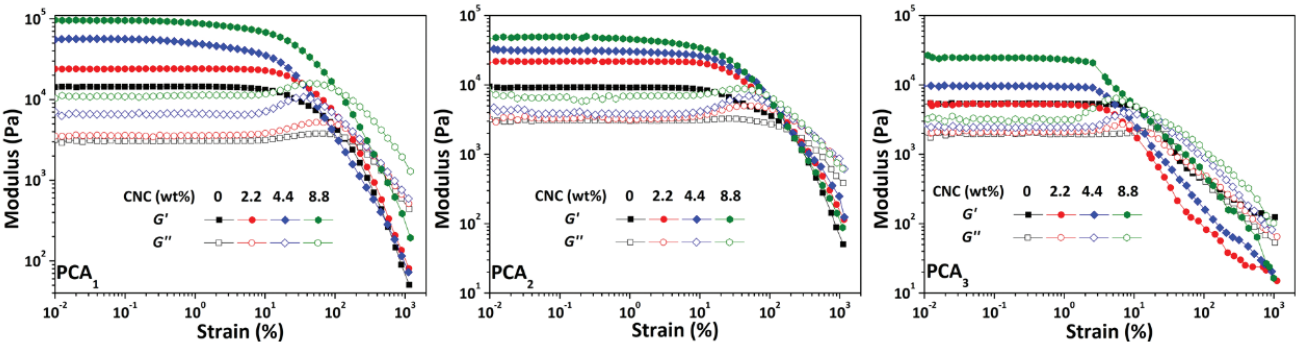

Figure 5. Strain sweep of PCA_1, PCA_2 and PCA_3 (20 wt%) with CNC of different concentrations

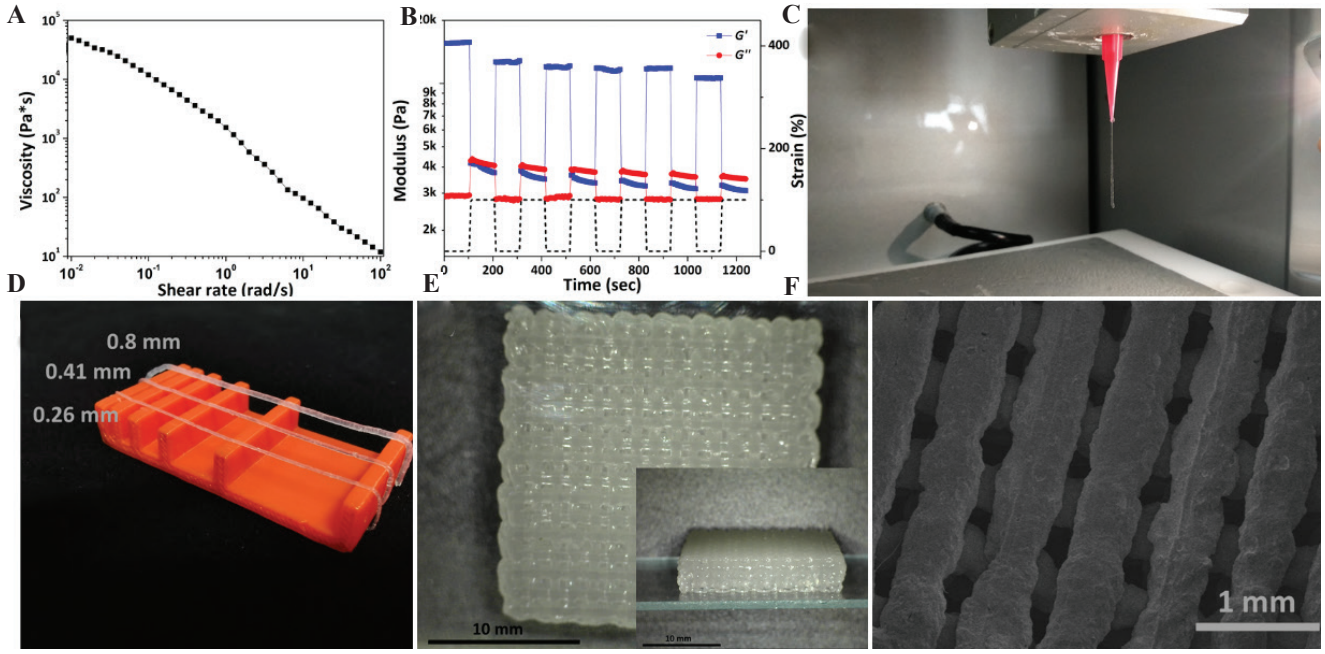

Figure 6. 3D printing results of hydrogels (20 wt% PCA_2+4.4 wt% cellulose nanocrystals). (A) Shear-thinning tests with the shear rate from 0.01 to 100 rad/s. (B) Shear recovery experiments with alternating strain of 0.01% and 100% (black dot line). (C) The extrusion effect. (D) Filament strength and stability with different size of nozzles. (E) The optical microscopic image of printed object and (F) The SEM image of printed object after lyophilization.

linear decline with the increase of the shear rate at 37°C. In addition, thixotropy, another critical parameter for the printable estimation, was also conducted to measure the recovery of the mechanical properties of materials under a large amplitude oscillatory force. The result (**Figure 6B**) indicated that this material has a typical elastic effect (***G'*** > ***G''***) under a small amplitude strain (γ=0.01%). When the strain is increased to a larger amplitude (γ=100%), ***G'*** decreases from 11 kPa to 3.6 kPa while ***G''*** increases from 2.8 kPa to 4.0 kPa, exhibiting a quasi-liquid state. Moreover, the gel modulus varied reciprocally with the variation of strain amplitude, showing that this material had a favorable irreversibility, that is, thixotropy.

Based on these results, extrusion-based 3D printing was conducted using Bio-architect®-PRO of Regenovo for further evaluation. Through adjusting the temperature in the cylinder to 37°C, the hydrogels could be extruded fluently as a filament rather than flowed as droplets (**Figure 6C**), intuitively demonstrating that the enhanced hydrogel has a required strength to be extruded. Then, filament collapse experiment was conducted using nozzles of syringe needles of different sizes for further confirmation (**Figure 6D**). It is seen that different thickness of filaments could hanged straight on different gap distance of scaffold, and no significant collapse can be observed, proving the favorable mechanical strength. By regulating the printing parameters (including size dimension, spacing distance, and translational speed), the material could be extruded and printed as a 3D hydrogel construct, as shown in **Figure 6E**. Under the optical microscope, the printed pattern showed relatively high resolution and fidelity with high layers (~4 mm), in which each filament was clearly visible without any obvious extrusion-swell or even collapse. Moreover, the details of printed constructs with different concentrations of inks are presented in **Table S1**. Meanwhile, the SEM image of the lyophilized 3D printed pattern clearly exhibited the intact structure and framework (**Figure 6F**). For the unmodified PCA_2 hydrogel (**Figure S1**), the printed structure was totally collapsed and lumped within 20 min based on our previous research[16]. So far, the results illustrate that the introduction of CNCs can effectively enhance the mechanical properties of the amorphous copolymers hydrogels, thereby significantly improving the extrudability and printability of the material.

3.5. *In vitro* cytotoxicity analysis

PCLA-PEG-PCLA-formed hydrogels were originally widely used as injectable hydrogels for drug delivery[40]. These materials show a good biocompatibility and biodegradability. Thus, fibroblasts were used to verify the former properties while lipase was used for the latter. The enzymatic degradation properties were displayed in **Figure S2**. The weight percent of hydrogel reduced linearly in 7-day incubation, showing a favorable biodegradability of the hydrogels. The *in vitro* cytotoxicity during the 3-day cultivation was characterized and estimated by live/dead staining assay. Under the fluorescent microscope

(**Figure 7**), it is found that the addition of PCLA-PEG-PCLA (5 mg/mL) did not influence the growth of fibroblasts and showed a similar growth tendency compared with blank control. Furthermore, CCK-8 assay was also used for the quantitative evaluation of the cell viability, as shown in **Figure 8**. Setting the absorbance result of blank control each day as 100%, it can be found that over 80% of viability of fibroblasts was maintained at a PCA_2 concentration of 5 mg/mL after co-cultivation for 24 h, and the viability increased further with a decrease

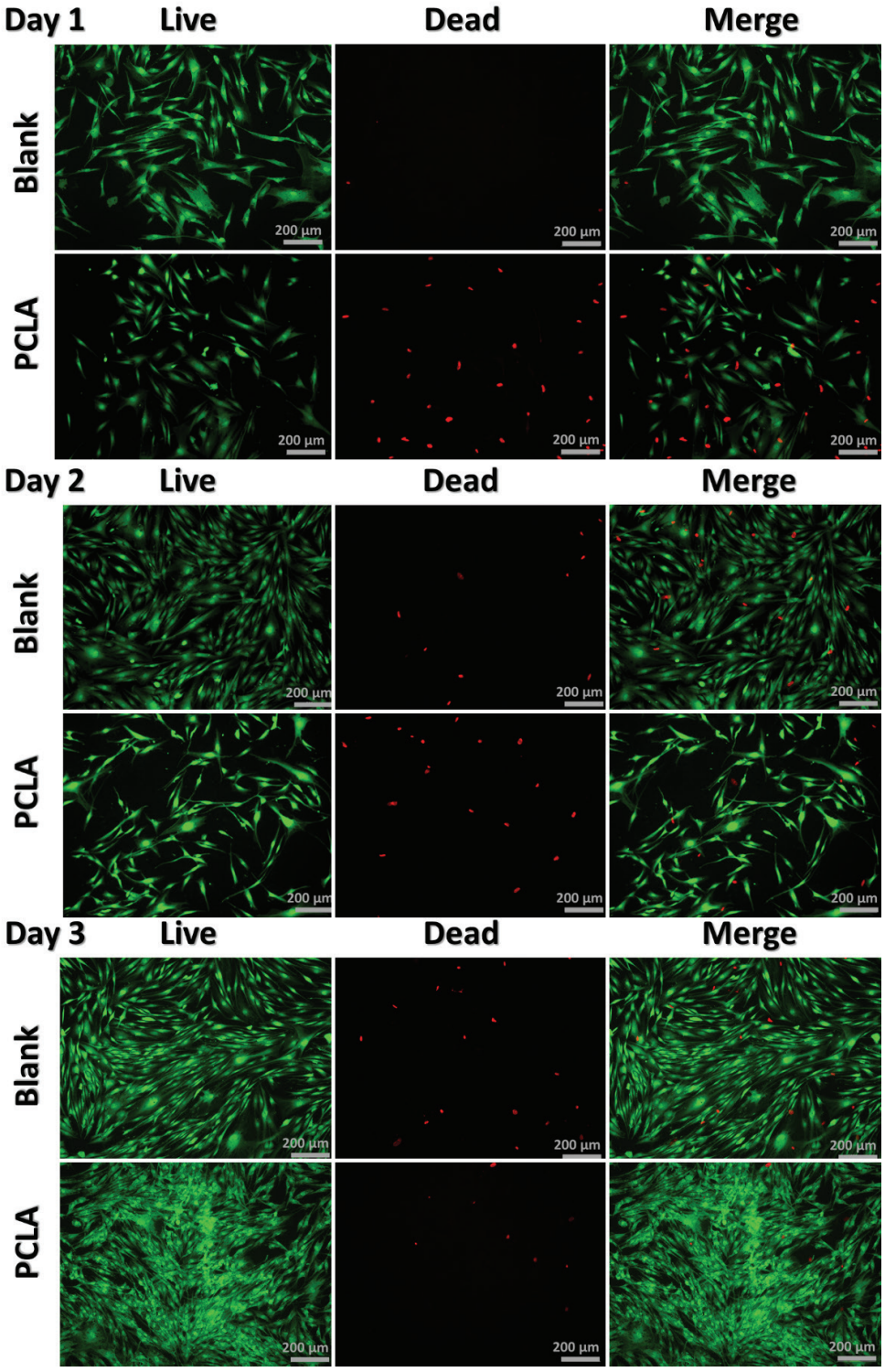

Figure 7. Fluorescent microscopic images of fibroblasts cultured with PCA_2 (5 mg/ml) and with medium only for 3 days.

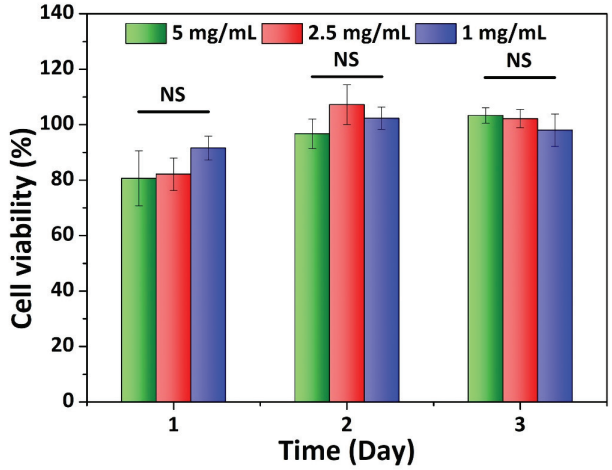

Figure 8. Cell viability of fibroblasts in the culture media after addition of PCA_2 at given concentrations as a function of days. The blank control with only culture medium each day was set as 100%. *n*=3.

of copolymer concentration. In the following 2 days, there was no significant difference between the additional PCA_2 of three different concentrations and blank control, showing around 100% cell viability. Meanwhile, the co-cultivation of hydrogel (20 wt% PCA_2+4.4 wt% CNC) with fibroblasts, which were seeded on the surface of the hydrogel, was also evaluated (**Figure S3**). The results exhibited a considerable cell compatibility after 12 h incubation and few dead cells were observed. All these results indicated that the addition of copolymers did not significantly affect the cell growth. However, none of living cells was observed in the encapsulated materials (unpublished data). It is speculated that the high printing pressure required for material with high viscosity may be detrimental to the cells. Therefore, we believe that as a bio-ink, the proper printing viscosity is as important as the biocompatibility of the material itself.

4. Conclusions

In this work, a series of PCLA-PEG-PCLA triblock amorphous block copolymers with different molecular weights and hydrophilic-hydrophobic ratios were prepared through ring-opening polymerization. CNCs of different concentrations were subsequently introduced into the copolymers formed hydrogels to investigate the improvement effect of the printability of the hydrogels. The results of thermodynamic and rheological studies show that the addition of CNC not only effectively enhances the thermal stability, forming a gel state at wider range of temperature, but also significantly increases the mechanical properties of hydrogels. When the CNC concentration reaches a certain level, the "sol-gel transition" presents at the sol system which cannot form a stable gel state at room temperature. The enhancement effect was proportional to CNC concentration within certain range. The printed 3D construct of CNC-enhanced copolymer formed hydrogels have strong mechanical properties to maintain the shape with high resolution and precision. These results proved that for the amorphous hydrogels, the printability of materials can be improved by adding rigid nanocrystals such as CNC. This method provides an effective approach of enhancing the comprehensive performance of materials for 3D bioprinting and other additive manufacturing technologies.

Acknowledgments

This work was financially supported by the National Key R&D Program of China (2017YFC1103400)..

Conflicts of interest

All authors declare that they have no conflict of interest.

Author contributions

Y. C. designed the experiments. Y. C., R. J., Y. Z., M. Y. and Y. Z. performed the experiments and analyzed the results. Y. C. wrote the manuscript. L. W. supervised the work and revised themanuscript.

References

1. Ng WL, Chua CK, Shen YF, 2019, Print Me An Organ! Why We Are Not There Yet. *Prog Polym Sci*, 97:101145. https://doi.org/10.1016/j.progpolymsci.2019.101145
2. Matai I, Kaur G, Seyedsalehi A, *et al.*, 2020, Progress in 3D Bioprinting Technology for Tissue/Organ Regenerative Engineering. *Biomaterials*, 226:119536. https://doi.org/10.1016/j.biomaterials.2019.119536
3. Murphy SV, Atala A, 2014, 3D Bioprinting of Tissues and Organs. *Nat Biotechnol*, 32:773–85. https://doi.org/10.1038/nbt.2958
4. Malda J, Visser J, Melchels FP, *et al.*, 2013, 25th Anniversary Article: Engineering Hydrogels for Biofabrication. *Adv Mater*, 25:5011–28. https://doi.org/10.1002/adma.201302042
5. Bedell ML, Navara AM, Du Y, *et al.*, 2020, Polymeric Systems for Bioprinting. *Chem Rev*, 120:10744–92.
6. Li X, Liu B, Pei B, *et al.*, 2020, Inkjet Bioprinting of Biomaterials. *Chem Rev*, 120:10793–833.
7. Valot L, Martinez J, Mehdi A, *et al.*, 2019, Chemical Insights Into Bioinks for 3D Printing. *Chem Soc Rev*, 48:4049–86. https://doi.org/10.1039/c7cs00718c
8. Zhang M, Vora A, Han W, *et al.*, 2015, Dual-Responsive Hydrogels for Direct-Write 3D Printing. *Macromolecules*,

48:6482–8.

9. Hoffman AS, 2012, Hydrogels for Biomedical Applications. *Adv Drug Deliv Rev*, 64:18–23.
10. Sponchioni M, Palmiero UC, Moscatelli D, 2019, Thermo-Responsive Polymers: Applications of Smart Materials in Drug Delivery and Tissue Engineering. *Mater Sci Eng C*, 102:589–605. https://doi.org/10.1016/j.msec.2019.04.069
11. Jungst T, Smolan W, Schacht K, *et al.*, 2016, Strategies and Molecular Design Criteria for 3D Printable Hydrogels. *Chem Rev*, 116:1496–539. https://doi.org/10.1021/acs.chemrev.5b00303
12. Nikolova MP, Chavali MS, 2019, Recent Advances in Biomaterials for 3D Scaffolds: A review. *Bioact Mater*, 4:271–92.
13. Zarrintaj P, Jouyandeh M, Ganjali MR, *et al.*, 2019, Thermo-Sensitive Polymers in Medicine: A Review. *Eur Polym J*, 117:402–23.
14. Drzewiecki KE, Parmar AS, Gaudet ID, *et al.*, 2014, Methacrylation Induces Rapid, Temperature-Dependent, Reversible Self-Assembly of Type-I Collagen. *Langmuir*, 30:11204–11. https://doi.org/10.1021/la502418s
15. Kajave NS, Schmitt T, Nguyen TU, *et al.*, 2020, Dual Crosslinking Strategy to Generate Mechanically Viable Cell-Laden Printable Constructs using Methacrylated Collagen Bioinks. *Mater Sci Eng C*, 107:110290. https://doi.org/10.1016/j.msec.2019.110290
16. Cui Y, Jin R, Zhou Y, *et al.*, 2021, Crystallization Enhanced Thermal-Sensitive Hydrogels of PCL-PEG-PCL Triblock Copolymer for 3D Printing. *Biomed Mater*, 16:035006. https://doi.org/10.1088/1748-605x/abc38e
17. Wang Z, An G, Zhu Y, *et al.*, 2019, 3D-Printable Self-Healing and Mechanically Reinforced Hydrogels With Host-Guest Non-Covalent Interactions Integrated into Covalently Linked Networks. *Mater Horiz*, 6:733–42. https://doi.org/10.1039/c8mh01208c
18. Yue K, Trujillo-de Santiago G, Alvarez MM, *et al.*, 2015, Synthesis, Properties, and Biomedical Applications of Gelatin Methacryloyl (GelMA) Hydrogels. *Biomaterials*, 73:254–71. https://doi.org/10.1016/j.biomaterials.2015.08.045
19. van den Bulcke AI, Bogdanov B, de Rooze N, *et al.*, 2000, Structural and Rheological Properties of Methacrylamide Modified Gelatin Hydrogels. *Biomacromolecules*, 1:31–8. https://doi.org/10.1021/bm990017d
20. Heinrich MA, Bansal R, Lammers T, *et al.*, 2019, 3D-Bioprinted Mini-Brain: A Glioblastoma Model to Study Cellular Interactions and Therapeutics. *Adv Mater*, 31:1806590. https://doi.org/10.1002/adma.201806590
21. Lim KS, Galarraga JH, Cui X, *et al.*, 2020, Fundamentals and Applications of Photo-Cross-Linking in Bioprinting. *Chem Rev*, 120:10662–94.
22. Billiet T, Gevaert E, de Schryver T, *et al.*, 2014, The 3D Printing of Gelatin Methacrylamide Cell-Laden Tissue-Engineered Constructs with High Cell Viability. *Biomaterials*, 35:49–62. https://doi.org/10.1016/j.biomaterials.2013.09.078
23. Colosi C, Shin SR, Manoharan V, *et al.*, 2016, Microfluidic Bioprinting of Heterogeneous 3D Tissue Constructs Using Low-Viscosity Bioink. *Adv Mater*, 28:677–84. https://doi.org/10.1002/adma.201503310
24. Moon RJ, Martini A, Nairn J, *et al.*, 2011, Cellulose Nanomaterials Review: Structure, Properties and Nanocomposites. *Chem Soc Rev*, 40:3941–94. https://doi.org/10.1039/c0cs00108b
25. Kargarzadeh H, Mariano M, Gopakumar D, *et al.*, 2018, Advances in Cellulose Nanomaterials. *Cellulose*, 25:2151–89. https://doi.org/10.1007/s10570-018-1723-5
26. Kontturi E, Laaksonen P, Linder MB, *et al.*, 2018, Advanced Materials through Assembly of Nanocelluloses. *Adv Mater*, 30:1703779. https://doi.org/10.1002/adma.201703779
27. Almeida AP, Canejo JP, Fernandes SN, *et al.*, 2018, Cellulose-Based Biomimetics and Their Applications. *Adv Mater*, 30:1703655. https://doi.org/10.1002/adma.201703655
28. Yang J, Han CR, Duan JF, *et al.*, 2012, Studies on the Properties and Formation Mechanism of Flexible Nanocomposite Hydrogels from Cellulose Nanocrystals and Poly (Acrylic Acid). *J Mater Chem*, 22:22467–80. https://doi.org/10.1039/c2jm35498e
29. Siqueira G, Kokkinis D, Libanori R, *et al.*, 2017, Cellulose Nanocrystal Inks for 3D Printing of Textured Cellular Architectures. *Adv Funct Mater*, 27:1604619. https://doi.org/10.1002/adfm.201604619
30. Yang J, Han CR, Duan JF, *et al.*, 2013, Mechanical and Viscoelastic Properties of Cellulose Nanocrystals Reinforced Poly (Ethylene Glycol) Nanocomposite Hydrogels. *ACS Appl Mater Interfaces*, 5:3199–207. https://doi.org/10.1021/am4001997
31. Ching YC, Ershad Ali M, Abdullah LC, *et al.*, 2016, Rheological Properties of Cellulose Nanocrystal-Embedded Polymer Composites: A Review. *Cellulose*, 23:1011–30.

https://doi.org/10.1007/s10570-016-0868-3

32. Ma T, Yang R, Zheng Z, *et al.*, 2017, Rheology of Fumed Silica/Polydimethylsiloxane Suspensions. *J Rheol*, 61:205–15. https://doi.org/10.1122/1.4973974
33. Song Y, Zheng Q, 2015, Linear Rheology of Nanofilled Polymers. *J Rheol*, 59:155–91.
34. Song Y, Zheng Q, 2016, A Guide for Hydrodynamic Reinforcement Effect in Nanoparticle-Filled Polymers. *Crit Rev Solid State Mater Sci*, 41:318–46. https://doi.org/10.1080/10408436.2015.1135415
35. Song Y, Zheng Q, 2016, Concepts and Conflicts in Nanoparticles Reinforcement to Polymers Beyond Hydrodynamics. *Prog Mater Sci*, 84:1–58.
36. Fan X, Xu H, Zhang Q, *et al.*, 2019, Insight into the Weak Strain Overshoot of Carbon Black Filled Natural Rubber. *Polymer*, 167:109–17. https://doi.org/10.1016/j.polymer.2019.01.076
37. Lu HD, Charati MB, Kim IL, *et al.*, 2012, Injectable Shear-Thinning Hydrogels Engineered with a Self-Assembling Dock-and-Lock Mechanism. *Biomaterials*, 33:2145–53. https://doi.org/10.1016/j.biomaterials.2011.11.076
38. Wang Q, Mynar JL, Yoshida M, *et al.*, 2010, High-Water-Content Mouldable Hydrogels by Mixing Clay and a Dendritic Molecular Binder. *Nature*, 463:339. https://doi.org/10.1038/nature08693
39. Olsen BD, Kornfield JA, Tirrell DA, 2010, Yielding Behavior in Injectable Hydrogels from Telechelic Proteins. *Macromolecules*, 43:9094–9. https://doi.org/10.1021/ma101434a
40. Zhang Z, Ni J, Chen L, *et al.*, 2011, Biodegradable and Thermoreversible PCLA-PEG-PCLA Hydrogel as a Barrier for Prevention of Post-Operative Adhesion. *Biomaterials*, 32:4725–36. https://doi.org/10.1016/j.biomaterials.2011.03.046